Symbiotic Communication Systems in the Internet of Things: A Framework for Double Adaptive Performance Analysis

Thai-Hoc Vu, Tien-Tung Nguyen, Tan N. Nguyen, *Senior Member, IEEE*, Lam-Thanh Tu, *Member, IEEE*, and Miroslav Voznak, *Senior Member, IEEE*

***Abstract*—This letter studies the performance enhancement of symbiotic systems, which begins by formulating a closed-form adaptive mutualism symbiotic strategy for the backscatter coefficient to achieve minimal decoding errors for both primary and secondary signals. Then, we analyze two scenarios: First, the primary source adapts the modulation scheme based on the channel conditions of the primary signal to meet the target bit error rate (BER), evaluating metrics: mode selection probability, outage mode probability (OMP), BER, and spectral efficiency. Second, the primary source adapts its transmission rate and/or power according to three channel policies: constant power with optimal rate adaptation, optimal simultaneous power and rate adaptation, and truncated channel inversion with a fixed rate. Results show that for the first scenario, our proposed approach significantly improves the OMP and BER of the adaptive symbiotic system in the moderate and high signal-to-noise ratio (SNR) regimes compared to the fixed one, while the second scenario shows a promising choice for balancing capacity between backscatter and cellular rates in the low SNR regime.**

***Index Terms*—Adaptive symbiotic radio, adaptive modulation, adaptive channel transmission, performance analysis.**

I. Introduction

SYMBIOTIC Radio (SR) represents a new approach for spectrum-efficient and energy-efficient communications, enabling network transmitters to use existing radio frequency signals through ambient backscatter [1]. Inspired by this breakthrough, SR has been studied in various contexts. For example, [2] developed an optimization strategy for the duration ratio between primary and secondary signals to improve mutual benefits in SR communications. Reference [3] provided closed-form expressions for outage probabilities and ergodic rates with non-orthogonal multiple access. Reference [4] explored finite block-length channel codes' effects on secondary transmissions, while [5] suggested a cell-free approach for SR communications to reduce interference and enhance network coverage.

Despite their advantages, SR systems still experience performance degradation in dynamic fading environments, challenging optimal operation in wireless communications. Historically, to mitigate the effects of fading, several adaptive transmission techniques have used channel estimation and receiver feedback. This allows for the adjustment of parameters such as transmit power, constellation size, symbol or bit rate, and coding type to better align with changing channel conditions [6]. Besides, realizing channel transmission policies [7] such as fixed power and rate adaptation (FPR), optimal power and rate adaptation (OPR), channel inversion with fixed rate (CIF), and truncated-channel inversion with fixed rate (TIF) is also a common intuition to achieve robust system performance, for example, in satellite-terrestrial relay networks [8] or aerial vehicle networks [9]. However, both strategy directions have remained unexplored within SR systems in existing studies [2], [3], [4], [5]. A key question is whether deploying adaptive transmission schemes in SR systems can indeed enhance system performance and energy efficiency.

To answer this question, we conduct a comprehensive analysis of using adaptive modulation and channel transmission schemes for adaptive mutualistic symbiotic systems. First, we design effective adaptive SR (ASR) systems, where backscatter devices adjust their backscatter coefficient to minimize decoding errors for both cellular signals and backscatter Internet-of-Things (IoT) information. Then, we improve adaptive SR systems by conducting two adaptive transmission schemes for cellular communications, including the following

- *Adaptive discrete modulation (ADM):* We focus on mode selection probability (MSP), outage mode probability (OMP), average spectral efficiency (ASE), and average bit-error rate (ABER).
- *Adaptive channel transmission (ACT):* We focus on the channel capacity of the FPR, OPR, and TIF schemes.

After detailing all the measures, i.e., deriving closed-form expressions/approximations, we provide qualitative numerical results to verify the correctness of the analytical results.

Notations: $F_X(\bullet)$ and $f_X(\bullet)$ are the respective cumulative probability function (CDF) and the probability density function (PDF). $\mathcal{CN}(0,\sigma^2)$ is the additive white Gaussian noise (AWGN) sample with zero mean and variance σ^2. $Q(x) = \frac{1}{\sqrt{2\pi}}\int_x^\infty \exp(-t^2/2)dt$ is the Gaussian function and $\mathbb{E}\{\bullet\}$ is the expectation operator, where $\Phi(\bullet)$, $\mathrm{Ei}(\bullet)$, $\Upsilon(\bullet,\bullet)$, $\Gamma(\bullet,\bullet)$, $\mathcal{K}_\bullet(\bullet)$, and $\mathcal{G}_{\cdot,\cdot}^{\cdot,\cdot}(\bullet|\cdots)$ represent the error, exponential integral,

Received 8 November 2025; accepted 5 December 2025. Date of publication 9 December 2025; date of current version 26 December 2025. This work was supported in part by the European Union under the REFRESH—Research Excellence for Region Sustainability and High-Tech Industries through the Operational Programme Just Transition under Project CZ.10.03.01/00/22_003/0000048, and in part by the Ministry of Education, Youth and Sports of the Czech Republic (MEYS CZ) within a Student Grant Competition in the VSB—Technical University of Ostrava under Project SGS SP2025/013. The associate editor coordinating the review of this article and approving it for publication was C. Tunc. *(Corresponding author: Lam-Thanh Tu.)*

Thai-Hoc Vu and Miroslav Voznak are with the Faculty of Electrical Engineering and Computer Science, VSB-Technical University of Ostrava, 70800 Ostrava, Czechia (e-mail: thai.hoc.vu@vsb.cz; miroslav.voznak@vsb.cz).

Tien-Tung Nguyen is with the Faculty of Electronics Technology, Industrial University of Ho Chi Minh City, Ho Chi Minh City 700000, Vietnam (e-mail: nguyentientung@iuh.edu.vn).

Tan N. Nguyen and Lam-Thanh Tu are with the Advanced Intelligent Technology Research Group, Faculty of Electrical and Electronics Engineering, Ton Duc Thang University, Ho Chi Minh City 70000, Vietnam (e-mail: nguyennhattan@tdtu.edu.vn; tulamthanh@tdtu.edu.vn).

Digital Object Identifier 10.1109/LWC.2025.3642143

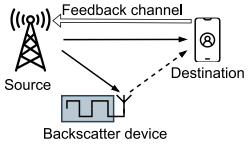

Fig. 1. Illustration of the considered system.

lower incomplete Gamma, upper incomplete Gamma, modified BesselK, and Meijer-G functions [10, eqs. (8.250.1), (8.211.1), (8.350.2), (8.432), and (9.301)], respectively.

II. System Model Description

As shown in Fig. 1, we study a downlink symbiotic system in a mutualistic relationship, including a source (S), a backscatter device (B) capable of signal processing, and one destination (D). All nodes experience Rayleigh fading channels,[1] and each is equipped with a single antenna. In this letter, D receives not only cellular information from S, but also IoT information from B. To negotiate the decoding between these two distinct signals in the symbiotic relationship, B cooperates with S to adaptively modulate its IoT signal using the radio frequency signal emitted by S and reflects it back to D. To do so, we consider the existence of an error-free feedback channel between S and D, which enables S to capture the quality of the S−D link, thus realizing the ADM or ACT technique, and assists B in setting its backscatter coefficient. This process occurs simultaneously with channel estimation for a short period of time before data exchange.

It is assumed that the perfect channel state information is available at the terminals [3], and the link coefficients between node $\mathrm{X} \in \{\mathsf{S}, \mathsf{B}\}$ and node $\mathrm{Y} \in \{\mathsf{B}, \mathsf{D}\}$ are indicated by h_{XY}. The signals received at D can be expressed as [3], [4], [5]

$$y_{\mathsf{D}} = \sqrt{P} h_{\mathsf{SD}} x_s + \sqrt{P}\sqrt{\rho} h_{\mathsf{SB}} h_{\mathsf{BD}} x_s x_b + n_{\mathsf{D}}, \tag{1}$$

where P is the transmit power, $x_s, x_b \sim \mathcal{CN}(0,1)$ are the source and backscatter symbols, ρ is the backscatter amplification coefficient,[2] and $n_{\mathsf{D}} \sim \mathcal{CN}(0, \sigma^2)$ is the AWGN sample.

From (1), the signal-to-interference-plus-noise ratio (SINR) of decoding x_s and x_b via an optimal successive interference cancelation mechanism can be derived, respectively, as

$$\gamma_s = \frac{|h_{\mathsf{SD}}|^2 \overline{\gamma}}{\rho |h_{\mathsf{SB}}|^2 |h_{\mathsf{BD}}|^2 \overline{\gamma} + 1}, \ \gamma_b = \rho |h_{\mathsf{SB}}|^2 |h_{\mathsf{BD}}|^2 \overline{\gamma}, \tag{2}$$

where $\overline{\gamma} \triangleq P/\sigma^2$ is the average signal-to-noise ratio (SNR).

Lemma 1: The strategy for negotiating the successful probability of decoding x_s and x_b at D can be defined as follows:

$$\rho^\star = \arg\max_{0<\rho} \min\{\gamma_s, \gamma_b\} = \frac{\left(\sqrt{1 + 4\overline{\gamma}|h_{\mathsf{SD}}|^2} - 1\right)}{2|h_{\mathsf{BD}}|^2 \overline{\gamma}}. \tag{3}$$

Proof: The problem of maximizing the minimum SINRs involves increasing the lowest SINR and decreasing the highest one until they are equal. Thus, solving $\gamma_s = \gamma_b$ yields

$$\begin{aligned} &|h_{\mathsf{SD}}|^2 \overline{\gamma} / \left(\rho |h_{\mathsf{SB}}|^2 |h_{\mathsf{BD}}|^2 \overline{\gamma} + 1\right) = \rho |h_{\mathsf{SB}}|^2 |h_{\mathsf{BD}}|^2 \overline{\gamma} \\ &\Rightarrow \rho^2 |h_{\mathsf{SB}}|^2 |h_{\mathsf{BD}}|^2 \overline{\gamma} + \rho - |h_{\mathsf{SD}}|^2 / \left(|h_{\mathsf{SB}}|^2 |h_{\mathsf{BD}}|^2\right) = 0 \\ &\Rightarrow \rho = \left(-1 \pm \sqrt{1 + 4\overline{\gamma}|h_{\mathsf{SD}}|^2}\right) / \left(2|h_{\mathsf{BD}}|^2 \overline{\gamma}\right). \end{aligned} \tag{4}$$

Due to $\rho > 0$ and $\sqrt{1 + 4\overline{\gamma}|h_{\mathsf{SD}}|^2} - 1 \geq 0$, one can achieve the final solution in (3). ■

When (3) is adopted, the end-to-end (e2e) SNR at D behaves

$$\overline{\gamma}_{\mathrm{e}} = \gamma_s(\rho^\star) = \gamma_b(\rho^\star) = \left(\sqrt{1 + 4\overline{\gamma}|h_{\mathsf{SD}}|^2} - 1\right)/2. \tag{5}$$

Since $|h_{\mathsf{SD}}|$ follows the Rayleigh distribution, $|h_{\mathsf{SD}}|^2$ is exponentially distributed on the scale $\Omega = \mathbb{E}\{|h_{\mathsf{SD}}|^2\}$. Thus, the respective CDF and PDF of $\overline{\gamma}_{\mathrm{e}}$ can be calculated as

$$\begin{aligned} F_{\overline{\gamma}_{\mathrm{e}}}(x) &= \Pr(\overline{\gamma}_{\mathrm{e}} < x) = F_{|h_{\mathsf{SD}}|^2}\left(\left(x^2 + x\right)/\overline{\gamma}\right) \\ &= 1 - \exp\left(-\left(x^2 + x\right)/(\Omega\overline{\gamma})\right), \end{aligned} \tag{6}$$

$$f_{\overline{\gamma}_{\mathrm{e}}}(x) = F'_{\overline{\gamma}_{\mathrm{e}}}(x) = \frac{2x+1}{\Omega\overline{\gamma}} \exp\left(-\frac{\left(x^2 + x\right)}{\Omega\overline{\gamma}}\right). \tag{7}$$

III. Adaptive Modulation Framework

The entire effective e2e SNR received at D is divided into $(K+1)$ non-overlapping intervals, and it is defined by a set of boundary values $\overline{\gamma}_\Sigma^0 = 0 < \overline{\gamma}_\Sigma^1 < \ldots < \overline{\gamma}_\Sigma^k < \ldots < \overline{\gamma}_\Sigma^K < \overline{\gamma}_\Sigma^{K+1} = +\infty$, where $k = 1, 2, \ldots, K$. D will arrange M_k-Phase-Shift Keying (PSK) modulations, with $M_k = 2^k$, from the K available options, ensuring that each scheme obtains the BER below the target BER_T. This information will then be sent back to S to establish the ADM. To avoid deep fades, the ADM is only active whenever the e2e instantaneous received SNR exceeds $\overline{\gamma}_\Sigma^1$, i.e., $k = 0$, no transmission mode (No-TX).

Next, we derive $\overline{\gamma}_\Sigma^k$ by solving the BER with Gray coding on the AWGN channel, i.e., $\mathsf{BER}_k(\overline{\gamma}_\Sigma^k) = \alpha_k Q([\beta_k \overline{\gamma}_\Sigma^k]^{\frac{1}{2}})$ [11, Eq. (9.50)], equal to the target BER_T, which yields,[3]

$$\overline{\gamma}_\Sigma^k = \frac{1}{\beta_k}\left[Q^{-1}\left(\frac{\mathsf{BER}_T}{\alpha_k}\right)\right]^2, \begin{cases} \alpha_k = 2/\log_2(M_k), \\ \beta_k = 2\sin^2(\pi/M_k). \end{cases} \tag{8}$$

A. Mode Selection Probability (MSP)

The MSP is defined as the probability that the mode $q = 0, \ldots, K$ is performed. The probability of mode q selected from $(K+1)$ possible modes can be expressed as

$$\mathsf{MSP}_q = \Pr\left(\overline{\gamma}_\Sigma^q \leq \overline{\gamma}_{\mathrm{e}} \leq \overline{\gamma}_\Sigma^{q+1}\right). \tag{9}$$

To proceed, let us rewrite the result in (9) as

$$\begin{aligned} \mathsf{MSP}_q &= \int_{\overline{\gamma}_\Sigma^q}^{\overline{\gamma}_\Sigma^{q+1}} f_{\overline{\gamma}_{\mathrm{e}}}(x)dx = \int_0^{\overline{\gamma}_\Sigma^{q+1}} f_{\overline{\gamma}_{\mathrm{e}}}(x)dx - \int_0^{\overline{\gamma}_\Sigma^q} f_{\overline{\gamma}_{\mathrm{e}}}(x)dx \\ &= F_{\overline{\gamma}_{\mathrm{e}}}\left(\overline{\gamma}_\Sigma^{q+1}\right) - F_{\overline{\gamma}_{\mathrm{e}}}\left(\overline{\gamma}_\Sigma^q\right). \end{aligned} \tag{10}$$

[1]Since Rayleigh fading is the worst-case scenario among fading models such as Rician and Nakagami-*m*, investigating the system in this model presents the worst performance limits in other fading environments [11].

[2]In practice, the operating range of ρ depends on the load impedance. For passive design, ρ is strictly bounded by $(0, 1)$. However, in active design that include amplifiers, ρ can appear larger than 1 because the device is injecting extra energy into the reflected signal [3], [4], [5], which is our focus.

[3]Note that the considered modulation scheme can also be extended to the case of M_k-ary Quadrature Amplitude Modulation (M-QAM) by reconfiguring the value of (α_k, β_k) such that $\alpha_k = 1, 2$ if $k = 1, 2$ and $\alpha_k = 4/k$ if $k \geq 3$ and $\beta_k = 2/k$ if $k = 1, 2$ and $\beta_k = 3/(2^k - 1)$ if $k \geq 3$ [11, Eq (9.31)]. On the other hand, we can achieve a mixed QAM and PSK modulation scheme by differentiating values of (α_k, β_k) in configuring $\overline{\gamma}_\Sigma^k$.

However, recall that $\overline{\gamma}_\Sigma^0 = 0$ and $\overline{\gamma}_\Sigma^{K+1} = +\infty$, and thus

$$\mathrm{MSP}_q = \begin{cases} F_{\overline{\gamma}_\mathrm{e}}(\overline{\gamma}_\Sigma^1), & q = 0, \quad (11a) \\ F_{\overline{\gamma}_\mathrm{e}}(\overline{\gamma}_\Sigma^{q+1}) - F_{\overline{\gamma}_\mathrm{e}}(\overline{\gamma}_\Sigma^q), & q \in [1, K-1], \quad (11b) \\ 1 - F_{\overline{\gamma}_\mathrm{e}}\left(\overline{\gamma}_\Sigma^K\right), & q = K. \quad (11c) \end{cases}$$

To gain insight into system design, let us evaluate $F_{\overline{\gamma}_\mathrm{e}}(x)$ in (6) at high SNR, that is, $\overline{\gamma} \to \infty$ and $\frac{1}{\overline{\gamma}} \to 0$. By using $1 - \exp(-z) \approx z$ for $z \to 0$, (6) is approximated as

$$F_{\overline{\gamma}_\mathrm{e}}(x) \overset{\overline{\gamma}\to\infty}{\approx} \left(x + x^2\right)/(\Omega\overline{\gamma}). \quad (12)$$

Herein, it is not difficult to recognize that if we let $1/\overline{\gamma} = 0$, $F_{\overline{\gamma}_\mathrm{e}}(x) = 0$. Combining this with (11), we can conclude that $\mathsf{MSP}_q \to 0$ with $q = 0, \ldots, (K-1)$ and $\mathsf{MSP}_q \to 1$ with $q = K$. This indicates that at high SNR, the system predominantly utilizes the highest modulation constellation.

B. Outage Mode Probability (OMP)

In wireless adaptive modulation, the OMP measures whether the receiving end can achieve the target BER, which corresponds to the initial transmission mode, i.e.,

$$\mathsf{OMP} = \Pr\left(\overline{\gamma}_\Sigma^0 \le \overline{\gamma}_\mathrm{e} \le \overline{\gamma}_\Sigma^1\right) = F_{\overline{\gamma}_\mathrm{e}}\left(\overline{\gamma}_\Sigma^1\right). \quad (13)$$

Based on (13) and (12), we conclude that the OMP is proportional to $\overline{\gamma}_\Sigma^1$. However, $Q'(x) = -\exp(-x^2/2)/\sqrt{2\pi} < 0$ indicates that $\mathsf{BER}_k(\overline{\gamma}_\Sigma^k)$ in (8) is a decreasing function of $\overline{\gamma}_\Sigma^k$, and the smaller the target BER, the larger the outage event.

C. Average Spectral Efficiency (ASE)

As the system uses K modulation levels, the ASE can be understood as the aggregate of data rates across all divided areas, adjusted by the probability of each event, i.e.,

$$\mathsf{ASE} = \sum\nolimits_{k=1}^{K} \mathsf{MSP}_k \log_2(M_k). \quad (14)$$

Since $\log_2(M_k) = \log_2(2^k) = k$ and $\overline{\gamma}_\Sigma^{K+1} = +\infty$, which leads to $F_{\overline{\gamma}_\mathrm{e}}(\overline{\gamma}_\Sigma^{K+1}) = 1$, the ASE in (14) can be rewritten as

$$\mathsf{ASE} = \sum\nolimits_{k=1}^{K} k\,\mathsf{MSP}_k = K - \sum\nolimits_{k=1}^{K} F_{\overline{\gamma}_\mathrm{e}}\left(\overline{\gamma}_\Sigma^k\right). \quad (15)$$

At high SNR regime, combining this result with (12) yields

$$\mathsf{ASE} \overset{\overline{\gamma}\to\infty}{\approx} K - \sum\nolimits_{k=1}^{K} \frac{1}{\Omega\overline{\gamma}} \overline{\gamma}_\Sigma^k \left(\overline{\gamma}_\Sigma^k + 1\right). \quad (16)$$

This result reveals that the maximum ASE value is determined by the highest modulation level K.

D. Average Bit-Error Rate (ABER)

Since the system operates with L modulation schemes, the ABER of the system is the average weight of the BERs associated with transmission [11, Eq. (9.72)], i.e.,

$$\mathsf{ABER} = \frac{\sum_{k=1}^{K} \mathsf{MSP}_k \mathsf{BER}_k}{\sum_{k=1}^{K} \mathsf{MSP}_k \log_2(M_k)}, \quad (17)$$

where the term BER_k can be derived from the BER formula with Gray coding as

$$\mathsf{BER}_k = \int_{\overline{\gamma}_\Sigma^k}^{\overline{\gamma}_\Sigma^{k+1}} \alpha_k\, Q\left(\sqrt{\beta_k x}\right) f_{\overline{\gamma}_\mathrm{e}}(x)\, dx. \quad (18)$$

To derive (17), we apply the integral-by-part with $u = Q(\sqrt{\beta_k x})$ and $dv = \int f_{\overline{\gamma}_\mathrm{e}}(x)\,dx$ to reshape the term (18) as

$$\mathsf{BER}_k = \alpha_k \left\{ Q\left(\sqrt{\beta_k \zeta}\right)[1 - F_{\gamma_\Sigma}(\zeta)] + \frac{\sqrt{\beta_k}}{2\sqrt{2\pi}} \times \int_0^\zeta [1 - F_{\gamma_\Sigma}(x)] \exp\left(-\frac{\beta_k}{2}x\right) \frac{1}{\sqrt{x}}\, dx \right\} \Bigg|_{\zeta=\overline{\gamma}_\Sigma^{k+1}}^{\zeta=\overline{\gamma}_\Sigma^k}. \quad (19)$$

As $\zeta \in \{\overline{\gamma}_\Sigma^k, k = 1, \ldots, (K-1)\}$, by inserting $F_{\overline{\gamma}_\mathrm{e}}(\bullet)$ in (6) into the above integral, defined as $\mathcal{I}$, we can rewrite it as

$$\mathcal{I} = \int_0^\zeta \frac{1}{\sqrt{x}} \exp\left(-\frac{x^2 + \theta x}{\Omega\overline{\gamma}}\right) dx, \ \theta = 1 + \Omega\overline{\gamma}\beta_k/2. \quad (20)$$

For $f(z) = \exp(-z)$ and its derivative of the n-th order $f^{(n)}(z) = (-1)^n \exp(-z)$, the Taylor series of $f(z)$ when mapping $z = (x^2 + \theta x)/(\Omega\overline{\gamma})$ and $z_0 = x^2/(\Omega\overline{\gamma})$ is given by

$$f(z) = f(z_0) + \sum\nolimits_{n=1}^{\infty} \frac{1}{n!} f^{(n)}(z_0)(z - z_0)^n = \exp\left(-\frac{x^2}{\Omega\overline{\gamma}}\right) + \sum\nolimits_{n=1}^{\infty} \frac{1}{n!} \exp\left(-\frac{x^2}{\Omega\overline{\gamma}}\right) \left[\frac{-\theta x}{\Omega\overline{\gamma}}\right]^n. \quad (21)$$

Following that, we can reformulate $\mathcal{I}$ and express it in closed-form expression using [10, eq. (3.381.8)] as

$$\mathcal{I} = \frac{1}{2}(\Omega\overline{\gamma})^{\frac{1}{4}} \Upsilon\left(\frac{1}{4}, \frac{\zeta^2}{\Omega\overline{\gamma}}\right) + \sum\nolimits_{n=1}^{\infty} \frac{(-1)^n}{n!} \left(\frac{\theta}{\Omega\overline{\gamma}}\right)^n \times (\Omega\overline{\gamma})^{\frac{2n+1}{4}} \Upsilon\left((2n+1)/4, \zeta^2/[\Omega\overline{\gamma}]\right)/2. \quad (22)$$

As $\zeta = \overline{\gamma}_\Sigma^{K+1} = +\infty$, introducing $t = \sqrt{x}$ converts $\mathcal{I}$ into

$$\mathcal{I} = 2\int_0^\infty \exp\left(-\frac{t^4}{\Omega\overline{\gamma}} - \frac{\theta t^2}{\Omega\overline{\gamma}}\right) dt = \sqrt{\theta} \exp\left(\theta^2/[8\Omega\overline{\gamma}]\right) \mathcal{K}_{1/4}\left(\theta^2/[8\Omega\overline{\gamma}]\right)/2, \quad (23)$$

which is derived using [10, eq. (3.323.3)].

IV. Adaptive Transmission Framework

A. Fixed Power and Rate Adaptation (FPR)

In conditions of rate adaptation with fixed transmit power and fluctuating channel strength, it is crucial to adjust the transmission rate to avoid exceeding the channel's capacity, ensuring smooth and efficient communication. The capacity in bit per second per Hertz (bps/Hz) can be expressed as

$$C_\mathrm{FPR} = \int_0^\infty \log_2(1 + x) f_{\overline{\gamma}_\mathrm{e}}(x)\, dx. \quad (24)$$

To calculate this term, we apply integral-by-part with $u = \ln(1 + x)$ and $dv = f_{\overline{\gamma}_\mathrm{e}}(x)\,dx$, and it returns that

$$C_\mathrm{FPR} = \frac{1}{\ln(2)} \int_0^\infty \frac{1}{x+1} \left[1 - F_{\overline{\gamma}_\mathrm{e}}(x)\right] dx. \quad (25)$$

After plugging $F_{\overline{\gamma}_\mathrm{e}}(\bullet)$ in (6) into (25), we employ the transformation $y = x^2 + x$ with variable and partial fraction relations

$$x = \left(\sqrt{1+4y} - 1\right)/2, \quad dy = \sqrt{1+4y}\,dx, \quad (26)$$

$$\frac{2}{\left(\sqrt{1+4y}+1\right)\sqrt{1+4y}} = \frac{2}{\sqrt{1+4y}} - \frac{2}{\sqrt{1+4y}+1}. \quad (27)$$

Afterward, the term C_FPR in (25) can be separated into

$$C_\mathrm{FPR} = \frac{1}{\ln(2)} \underbrace{\int_0^\infty \frac{2}{\sqrt{1+4y}} \exp\left(-\frac{y}{\Omega\overline{\gamma}}\right) dy}_{\mathcal{K}_1} \quad (28)$$

$$-\frac{1}{\ln(2)}\underbrace{\int_0^{\infty}\frac{2}{\sqrt{1+4y}+1}\exp\left(-\frac{y}{\Omega\overline{\gamma}}\right)dy}_{\mathcal{K}_2}.$$

Now, we can utilize [10, Eq. (3.362.2)] for $\mathcal{K}_1$, which returns

$$\mathcal{K}_1=\sqrt{\pi\Omega\overline{\gamma}}\exp(1/[4\Omega\overline{\gamma}])\left[1-\Phi\left(1/\left[2\sqrt{\Omega\overline{\gamma}}\right]\right)\right]. \quad (29)$$

Meanwhile, we derive $\mathcal{K}_2$ using the identity [12, Eq. (8.3.1.1)]

$$\frac{1}{\sqrt{1+x}+1}=\frac{1}{2}\frac{1}{\sqrt{\pi}}\,x\,\mathcal{G}_{2,2}^{1,2}\left(x\middle|\begin{matrix}-\frac{1}{2},-1\\-1,-2\end{matrix}\right), \quad (30)$$

and then applying the aid of [10, 7.813.1] to get the solution

$$\mathcal{K}_2=\frac{4}{\sqrt{\pi}}\left(\frac{1}{\Omega\overline{\gamma}}\right)^{-2}\mathcal{G}_{3,2}^{1,3}\left(4\Omega\overline{\gamma}\middle|\begin{matrix}-1,-\frac{1}{2},-1\\-1,-2\end{matrix}\right). \quad (31)$$

B. Optimal Power and Rate Adaptation (OPR)

When feedback channel conditions from D to S via an error-free feedback link are favorable (i.e., large $\overline{\gamma}_{\mathrm{e}}$), higher power and rates are allocated. Conversely, these parameters are reduced under unfavorable conditions (i.e., small $\overline{\gamma}_{\mathrm{e}}$). Thus, the capacity in bps/Hz can be defined as in [11, Eq. (9.17)] as

$$C_{\mathrm{OPR}}=\int_{\gamma_c}^{\infty}\log_2(x/\gamma_c)f_{\overline{\gamma}_{\mathrm{e}}}(x)\,dx, \quad (32)$$

where γ_c denotes the ideal cutoff SNR threshold, at which data transmission over the network is stopped, and it follows:

$$\int_{\gamma_c}^{\infty}\left(\frac{1}{\gamma_c}-\frac{1}{x}\right)f_{\overline{\gamma}_{\mathrm{e}}}(x)\,dx=1. \quad (33)$$

And, the probability that the system stops is measured by

$$\mathrm{OP}_{\mathrm{OPR}}=\Pr(\overline{\gamma}_{\mathrm{e}}<\gamma_c)=F_{\gamma_\Sigma}(\gamma_c). \quad (34)$$

With integral-by-part, we rewrite the capacity in (32) as

$$\begin{aligned}C_{\mathrm{OPR}}&=\int_{\gamma_c}^{\infty}\frac{1}{\ln(2)x}\left[1-F_{\overline{\gamma}_{\mathrm{e}}}(x)\right]dx\\&=\frac{1}{\ln(2)}\int_{\gamma_c}^{\infty}\frac{1}{x}\exp\left(-\frac{x^2+x}{\Omega\overline{\gamma}}\right)dx, \quad (35)\end{aligned}$$

where the last integral is reformulated using $F_{\overline{\gamma}_{\mathrm{e}}}(\bullet)$ in (6).

To derive C_{OPR}, we make use of $y=(x^2+x)$ with $\tau=\gamma_c(\gamma_c+1)$, variable changes in (26), and a partial fraction

$$\frac{1}{(\sqrt{1+4y}-1)\sqrt{1+4y}}=\frac{1}{\sqrt{1+4y}-1}-\frac{1}{\sqrt{1+4y}}, \quad (36)$$

which returns the two following integrals

$$\begin{aligned}C_{\mathrm{OPR}}=&\frac{1}{\ln(2)}\underbrace{\int_{\tau}^{\infty}\frac{2}{\sqrt{1+4y}-1}\exp\left(-\frac{y}{\Omega\overline{\gamma}}\right)dy}_{\mathcal{A}_1}\\&-\frac{1}{\ln(2)}\underbrace{\int_{\tau}^{\infty}\frac{2}{\sqrt{1+4y}}\exp\left(-\frac{y}{\Omega\overline{\gamma}}\right)dy}_{\mathcal{A}_2}. \quad (37)\end{aligned}$$

Here, we solve the term $\mathcal{A}_2$ by applying $t=1+4y$ in combination with [10, Eq. (3.381.9)], and it returns

$$\mathcal{A}_2=\exp(1/[4\Omega\overline{\gamma}])\sqrt{\Omega\overline{\gamma}}\,\Gamma(1/2,(1+4\tau)/[4\Omega\overline{\gamma}]). \quad (38)$$

Meanwhile, we solve $\mathcal{A}_1$ by applying the partial fraction

$$\frac{2}{\sqrt{1+4y}-1}=\frac{1}{2y}+\frac{1}{2y}\sqrt{1+4y}, \quad (39)$$

which returns a new relation as follows:

$$\begin{aligned}\mathcal{A}_1&=\int_{\tau}^{\infty}\frac{\sqrt{1+4y}}{2y}\exp\left(-\frac{y}{\Omega\overline{\gamma}}\right)dy+\int_{\tau}^{\infty}\exp\left(-\frac{y}{\Omega\overline{\gamma}}\right)\frac{dy}{2y}\\&=\underbrace{\int_{\tau}^{\infty}\frac{\sqrt{1+4y}}{2y}\exp\left(-\frac{y}{\Omega\overline{\gamma}}\right)dy}_{\mathcal{L}}-\frac{1}{2}\mathrm{Ei}\left(-\frac{\tau}{\Omega\overline{\gamma}}\right), \quad (40)\end{aligned}$$

where the last term is derived using [10, Eq. (3.351.4)].

To solve $\mathcal{L}$, let us define $g(z)=\sqrt{z}=z^{\frac{1}{2}}$. Then, we can deduce the n-th order derivative of $g(z)$, with $n\geq 1$, as

$$g^{(n)}(z)=(-1)^{n-1}\,z^{-\frac{2n-1}{2}}\,\frac{1}{2}\prod_{l=1}^{n-1}\left(\frac{2l-1}{2}\right). \quad (41)$$

Mapping $z=1+4y$ and $z_0=4y$ gives us a Taylor series

$$g(z)=2\sqrt{y}+\sum_{n=1}^{\infty}\frac{(-1)^{n-1}}{2^{2n}n!}\prod_{l=1}^{n-1}\left(\frac{2l-1}{2}\right)y^{-\frac{2n-1}{2}}. \quad (42)$$

Afterward, we inject this result into $\mathcal{L}$ to get that

$$\begin{aligned}\mathcal{L}=&\int_{\tau}^{\infty}\frac{1}{\sqrt{y}}\exp\left(-\frac{y}{\Omega\overline{\gamma}}\right)dy+\sum_{n=1}^{\infty}\frac{(-1)^{n-1}}{2^{2n}n!}\prod_{l=1}^{n-1}\left(\frac{2l-1}{2}\right)\\&\times\frac{1}{2}\int_{\tau}^{\infty}\frac{1}{y^{n+\frac{1}{2}}}\exp\left(-\frac{y}{\Omega\overline{\gamma}}\right)dy\\=&\sqrt{\Omega\overline{\gamma}}\,\Gamma\left(\frac{1}{2},\frac{\tau}{\Omega\overline{\gamma}}\right)+\sum_{n=1}^{\infty}\frac{(-1)^{n-1}}{2^{2n+1}n!}\prod_{l=1}^{n-1}\left(\frac{2l-1}{2}\right)\\&\times(\Omega\overline{\gamma})^{1/2-n}\,\Gamma(1/2-n,\tau/[\Omega\overline{\gamma}]), \quad (43)\end{aligned}$$

where the last term is derived using [10, Eq. (3.381.9)].

To derive γ_c, we rewrite (33) using $f_{\overline{\gamma}_{\mathrm{e}}}(\bullet)$ in (7) as

$$\begin{aligned}&\Leftrightarrow\frac{\left[1-F_{\overline{\gamma}_{\mathrm{e}}}(\gamma_c)\right]}{\gamma_c}-\int_{\gamma_c}^{\infty}\exp\left(-\frac{x^2+x}{\Omega\overline{\gamma}}\right)\frac{2x+1}{x\Omega\overline{\gamma}}\,dx=1\\&\Leftrightarrow\left[1-F_{\overline{\gamma}_{\mathrm{e}}}(\gamma_c)\right]/\gamma_c-\frac{1}{\Omega\overline{\gamma}}\mathcal{A}_1=1, \quad (44)\end{aligned}$$

which can be solved numerically due to the involvement of complicated and special functions in the formulation of $\mathcal{A}_1$.

C. Truncated-Channel Inversion With Fixed Rate (TIF)

To maintain a steady received SNR while minimizing capacity loss over other techniques, the source adjusts its transmission power in response to channel fading when $\overline{\gamma}_{\mathrm{e}}>\gamma_0$ is met. The channel capacity is expressed as in [9, Eq. (33)] as

$$C_{\mathrm{TIF}}=\log_2\left(1+\left[\int_{\gamma_0}^{\infty}\frac{f_{\overline{\gamma}_{\mathrm{e}}}(x)\,dx}{x}\right]^{-1}\right)\Pr(\overline{\gamma}_{\mathrm{e}}>\gamma_0), \quad (45)$$

where γ_0 is chosen so that a specified outage probability is satisfied, or alternatively, C_{TIF} is maximized. Injecting (7) into (45), followed by the same method for $\mathcal{A}_1$, we achieve

$$C_{\mathrm{TIF}}=\log_2\left(1+(\mathcal{A}_1(\gamma_c\leftarrow\gamma_0)/(\Omega\overline{\gamma}))^{-1}\right)\left[1-F_{\overline{\gamma}_{\mathrm{e}}}(\gamma_0)\right]. \quad (46)$$

V. Numerical Results and Discussions

This section validates the efficacy of the developed theories versus Monte Carlo simulations with 10^5 channel samples.

We begin with the MSP versus SNR $\overline{\gamma}$ in Fig. 2(a), where we see that mode 1 ($q=0$) and mode 4 ($q=3$) dominate in the low and high SNR regimes, respectively, and this partially

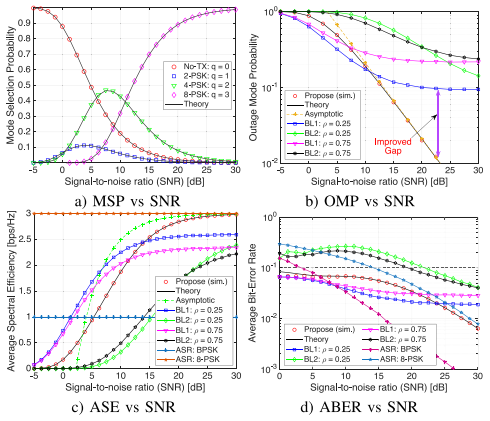

Fig. 2. ASR with ADM under $K = 3$ and $\mathsf{BER}_T = 10^{-1}$. The formula in (22) requires 10 terms in the Taylor series. In comparison, fixed SR systems employ two ADM baselines (BLs): BL1 ($\overline{\gamma}_{\mathrm{e}} = \gamma_s$) and BL2 ($\overline{\gamma}_{\mathrm{e}} = \min\{\gamma_s, \gamma_b\}$), with $\Omega = 1.5$, $\mathbb{E}\{|h_{\mathsf{SB}}|^2\} = 0.5$, $\mathbb{E}\{|h_{\mathsf{BD}}|^2\} = 1$.

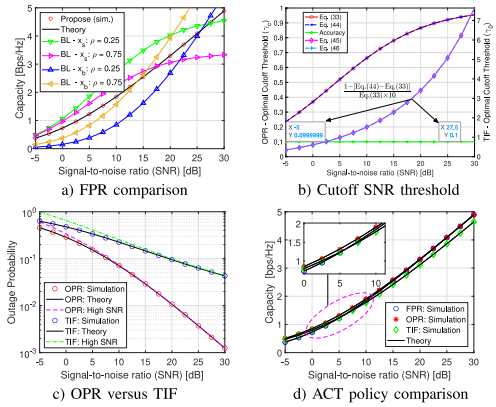

Fig. 3. ASR using ACT. The formula in (43) only requires 2 terms in the Taylor series to ensure the convergence.

conforms to the asymptotic analysis of the CDF of $\overline{\gamma}_{\mathrm{e}}$. Next, the OMP of decoding x_s is plotted by Fig. 2(b), which shows that BL1 dominates at low SNR, but this trend is reversed at the other regimes, where our proposed solution is the best due to a linear SNR improvement. In contrast, both BL1 and BL2 appear on the performance floor at high SNR, and the variation of the coefficient ρ causes an increase in their OMPs. The rationale behind such phenomena is that the higher the value $\overline{\gamma}$ or ρ, the higher the interference caused by the backscatter signal. Similarly, there is an equivalent trend for the ASE performance in Fig. 2(c) and the ABER performance in Fig. 2(d), with a slight difference in that all schemes seem to reach the ASE floor at high SNR, equal to the largest modulation level, and using BL1 violates the target BER due to the dominant of the backscatter signals.

Next, we turn our focus to the capacity analysis of the FPR and fixed SR systems with the SINRs in (2), where Fig. 3(a) shows that our proposed adaptive system achieves a well-balanced capacity performance between the primary and secondary signals. Fig. 3(b) explores the optimal cut-off SNR thresholds for both OPR and TIF. As observed, the method we examine, a two-term Taylor series approximation, produces a cut-off threshold that aligns closely with the integral-based definition, achieving an accuracy of 99%. Furthermore, the cutoff threshold for OPR is restricted within $[0, 1]$, while TIF dynamically adjusts its threshold to maximize channel capacity, resulting in a linear dependence on $\overline{\gamma}$. However, this capacity optimization introduces a trade-off in outage performance, as plotted in Fig. 3(c), where the OPR shows the performance much better than the TIF. Unfortunately, the advance of TIF remains negligible, as evidenced in Fig. 3(d), where TIF achieves capacity levels comparable to OPR and even slightly exceeds FPR under low SNR conditions. This trend reverses in moderate and high SNR regimes, where FPR's capacity approaches that of OPR, and TIF falls behind both. In particular, to reach the same target capacity, TIF requires a transmit SNR approximately 1.5 dB higher than that of FPR and OPR.

VI. Conclusion

This letter investigated the feasibility of ADM and ACT methods in adaptive symbiotic systems while providing closed-form exact and approximate expressions for performance evaluations. Our analyzes provided several useful insights into the system designs and new key findings in performance improvements. However, there are still many points that should be further investigated in future studies, for example, energy consumption, hardware impairments, imperfect SIC, multi-antenna nodes, cell-free, reconfigurable surfaces, finite blocklength, and especially, this letter can serve as a benchmark for future deep learning-based solutions.

References

[1] R. Long et al., "Symbiotic radio: A new communication paradigm for passive Internet of Things," *IEEE Internet Things J.*, vol. 7, no. 2, pp. 1350–1363, Feb. 2020.

[2] Q. Zhang et al., "Mutualistic mechanism in symbiotic radios: When can the primary and secondary transmissions be mutually beneficial?" *IEEE Trans. Wireless Commun.*, vol. 21, no. 10, pp. 8036–8050, Oct. 2022.

[3] Q. Zhang et al., "Backscatter-NOMA: A symbiotic system of cellular and Internet-of-Things networks," *IEEE Access*, vol. 7, pp. 20000–20013, 2019.

[4] Z. Chu et al., "Resource allocations for symbiotic radio with finite blocklength backscatter link," *IEEE Internet Things J.*, vol. 7, no. 9, pp. 8192–8207, Sep. 2020.

[5] Z. Dai et al., "Rate-region characterization and channel estimation for cell-free symbiotic radio communications," *IEEE Trans. Commun.*, vol. 71, no. 2, pp. 674–687, Feb. 2023.

[6] T. Nechiporenko et al., "Performance of optimum switching adaptive *M*-QAM for amplify-and-forward relays," *IEEE Trans. Veh. Technol.*, vol. 58, no. 5, pp. 2258–2268, Jun. 2009.

[7] M.-S. Alouini and A. J. Goldsmith, "Capacity of Rayleigh fading channels under different adaptive transmission and diversity-combining techniques," *IEEE Trans. Veh. Technol.*, vol. 48, no. 4, pp. 1165–1181, Jul. 1999.

[8] K. An and T. Liang, "Hybrid satellite-terrestrial relay networks with adaptive transmission," *IEEE Trans. Veh. Technol.*, vol. 68, no. 12, pp. 12448–12452, Dec. 2019.

[9] R. Polus and C. D'Amours, "Capacity analysis of UAV-to-ground channels with shadowing: Power adaptation schemes and effective capacity," *IEEE Open J. Veh. Technol.*, vol. 5, pp. 71–77, 2023.

[10] A. Jeffrey and D. Zwillinger, *Table of Integrals, Series, and Products*. Amsterdam, The Netherlands: Elsevier, 2007.

[11] A. Goldsmith, *Wireless communications*. Cambridge, U.K.: Cambridge Univ. Press, 2005.

[12] Y. A. Brychkov, *Handbook of Special Functions: Derivatives, Integrals, Series and Other Formulas*. Boca Raton, FL, USA: Chapman and Hall/CRC, 2008.